

# STUDY OF HYPERFRAGMENTS

## Part V. Analysis of Light Hyperfragments

BY K. N. CHAUDHARI, S. N. GANGULI, N. K. RAO AND M. S. SWAMI\*

(Tata Institute of Fundamental Research, Bombay, India)

Received September 28, 1966

(Communicated by Dr. R. R. Daniel, F.A.Sc.)

### ABSTRACT

464 non-mesic and 65 mesic decay of hyperfragments (HFs) produced by pions of momenta 3.5 GeV/c. and 17.2 GeV/c. and protons of momentum 23 GeV/c., have been used to obtain information on  $Q^-$ , the ratio of non-mesic to  $\pi^-$  mesic events and  $S$ , the ratio of neutron to proton stimulated events as a function of charge of HFs.  $Q^-$  is found to increase rapidly with the increase in charge of HFs; the value of  $Q^-$  for HFs of  $Z \geq 3$  is  $14.6 \pm 3.0$  which is high compared to the theoretical value of about 4 to 5. The value of  $S$  is found to be  $> 1$  for all HFs of  $Z \geq 2$ .

### 1. INTRODUCTION

THE common decay modes of hyperfragments (HFs) are: (i) mesic decay (MHFs) in which a pion is emitted, and (ii) non-mesic decay (NMHFs) in which no pion is emitted. The latter decay mode is predominantly due to the interaction of  $\Lambda$  with a single nucleon which can be written as:



Reaction (1) is called the stimulation of  $\Lambda$  by a proton and reaction (2) is called the stimulation of  $\Lambda$  by a neutron. The experimentally determinable parameters in the decay of HFs are:

$$(a) Q^- = \frac{\text{number of NMHFs}}{\text{number of MHFs that decay by } \pi^- \text{ mode}}$$

$$(b) S = \frac{\text{number of NMHFs that decay without emission of fast proton}}{\text{number of NMHFs that decay with emission of fast protons}}$$

---

\* Now at the Physics Department of Punjab University, Chandigarh, India, on deputation from the Tata Institute of Fundamental Research.

In case (b), fast protons are defined as those that have energy  $\geq 30$  MeV; this energy criterion removes the unwanted contribution of charged particles due to evaporation of the HF core nucleus.

In order to understand the  $\Lambda$ -nucleon interaction it is of importance to investigate experimentally the ratios  $Q^-$  and  $S$  as a function of charge and mass of HFs. These ratios have been theoretically calculated by Dalitz<sup>1</sup> and Ferrari and Fonda<sup>2</sup> respectively; a comparison of the theoretical values with those of the experiment will provide valuable information on  $\Lambda$ -nucleon interaction. Since accurate mass or charge determination is not possible for short-range HFs, we have selected for this investigation only those HFs that have ranges  $> 20 \mu\text{m}$ .

## 2. EXPERIMENTAL DETAILS AND RESULTS

### 2.1. Details of the Stacks

Three nuclear emulsion stacks A, B and C which were exposed to beams of 3.5 GeV/c. pions, 23 GeV/c. protons and 17.2 GeV/c. pions respectively have been used in this investigation. The details regarding the stacks, scanning and selection criteria of HFs are described in Parts I, II and IV<sup>3-5</sup> of this series.

For accurate analysis of the events, it is necessary to know the shrinkage factor and stopping power of the emulsions. These have been obtained in the following way:

*Stacks B and C.*—The thickness of emulsions in stacks B and C were measured before and after processing of the stacks; therefore the shrinkage factor for these emulsions was known. Stopping powers of stacks B and C were determined by measuring in each the ranges of 50 flat  $\mu^+$  arising from  $\pi^+$  decay at rest. The mean ranges of  $\mu^+$  in these two stacks were found to be  $601.4 \pm 3.5 \mu\text{m}$  and  $605.0 \pm 3.0 \mu\text{m}$  respectively. These are in good agreement with the mean range of  $602.2 \pm 1.5 \mu\text{m}$ ,<sup>6</sup> obtained for  $\mu^+$  in a standard emulsion of density 3.815 gm./cm.<sup>3</sup>

*Stack A.*—The original thicknesses of the emulsion pellicles of stack A were not known. Therefore the shrinkage factor and the stopping power were determined by 'regression method' of Fry and White<sup>7</sup> using 50  $\mu^+$  from decay of  $\pi^+$  mesons at rest. With this method, the mean range of  $\mu^+$  was found to be  $612 \pm 5 \mu\text{m}$ ; this value lies within two-standard deviation for the  $\mu^+$  range in a standard emulsion.

Since the stopping powers for the three stacks A, B and C are in agreement with that of a standard emulsion, the range-energy relations given by Heckman *et al.*<sup>8</sup> for standard emulsion were used throughout.

## 2.2. Selection of Events

A total of 1173 HFs were obtained in the three stacks. From this we have selected those HFs that have ranges  $> 20 \mu\text{m}$ . With this procedure we have obtained in all 464 NMHFs and 67 MHFs. The number of black and grey tracks ( $N_h$ ) associated with each parent star containing the HF was determined. From the  $N_h$  distribution of these stars, it was concluded that more than 90% of the HFs were produced in disintegrations of heavy nuclei (Ag, Br) of emulsion.

Data collected on the range distribution of HFs as a function of range for various incident beams<sup>9-11</sup> including the results from the present investigation are given in Table I. It can be seen from this table that as the energy of the incident beam increases the fraction of long range HFs also increases. This clearly brings out the advantage of working with high energy incident beams which result in easier identification of HFs.

TABLE I

*Ranges of hyperfragments (in percentage) for different incident beams*

Incident beam	Percentage of HFs with range			
	0-10 $\mu\text{m}$	10-20 $\mu\text{m}$	20-50 $\mu\text{m}$	$> 50 \mu\text{m}$
Stopping $\text{K}^{-9}$	61.6*	10.0	11.6	16.8
0.8 GeV/c. $\text{K}^{-10}$	85.0	2.6	3.4	9.0
3.0 GeV/c. $\text{K}^{-11}$	74.4	6.0	5.5	14.1
5.0 GeV/c. $\text{K}^{-11}$	72.9	6.5	6.7	13.9
3.5 GeV/c. $\pi^-$	67.6	11.9	9.1	11.4
17.2 GeV/c. $\pi^-$	36.3	13.2	17.8	32.7
23 GeV/c. P	35.0	14.3	20.0	30.7

\* HFs of range  $\leq 1 \mu\text{m}$  are not included in this.

### 2.3. Mass determination of Particles from Decay of HFs

All tracks from decay of HFs were followed till they were brought to rest, left the stack or interacted in flight. Identification of pions from decay of HFs was made from the variation in grain density and Coulomb scattering along their tracks. In this way all the MHFs were identified. In NMHF events mass measurements were made on all fast charged particles of residual range  $\geq 4$  mm. and which subtended dip-angles  $\leq 30^\circ$  with respect to the plane of emulsion; there were 57 such tracks. In these cases mass measurements were carried out by the constant Sagitta scattering method for stopping particles; the scheme used was P ( $0.7 \mu\text{m}$ ). From a comparison of these data with similar measurements made on well-identified protons, it is found that all the 57 fast-charged particles except 2 are due to protons; these two tracks could be due to deuterons or tritons (the details regarding this type of measurement is described in Part III.<sup>12</sup> Thus we conclude that the contribution of deuterons and tritons among the fast-charged particles of range  $\geq 4$  mm. is  $\lesssim 4\%$ .

### 2.4. Charge Spectrum of HFs

The charge of a particle producing a track of range  $> 20 \mu\text{m}$  can be found in two ways: (a) by track width measurement and (b) by visual inspection. They are described below.

(a) *Track-width method.*—Track-width measurements have been made on well identified flat (dip-angle  $\leq 10^\circ$ ) protons, alpha-particles,  $\text{Li}^8$  and  $\text{B}^8$  tracks. The variation of track-width as a function of residual range is shown in Fig. 1 (a). The variation of track-width with dip-angle of the tracks of  $\text{Li}^8$  fragments of range  $60 \mu\text{m}$  is shown in Fig. 1 (b). From Fig. 1 it is clear that the average track-width for tracks of dip-angles  $\leq 25^\circ$  remains constant. With this method we have made track-width measurements on all tracks of HFs, whose dip-angles were  $\leq 25^\circ$ . The typical errors involved in the charge

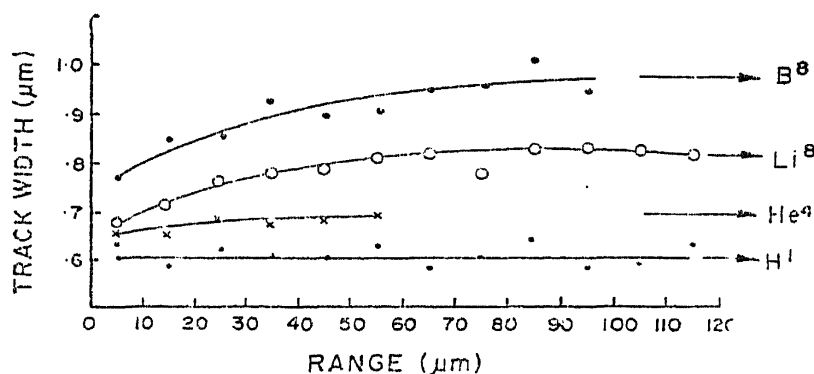


FIG. 1. (a) Track-width versus residual range for protons, alphas,  $\text{Li}^8$  and  $\text{B}^8$  tracks.

estimation by this method are: (i) 0.5 charge unit for tracks of range  $> 60 \mu\text{m}$  and (ii) 1.0 charge unit for tracks in the range interval  $20\text{--}60 \mu\text{m}$ .

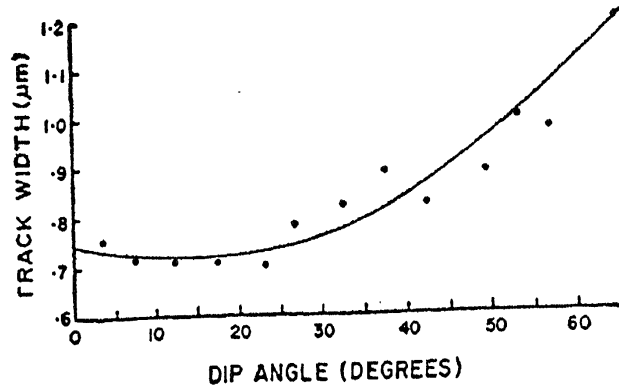


FIG. 1. (b) Variation of track-width, for  $\text{Li}^8$ s of range =  $60 \mu\text{m}$ , as a function of dip-angle.

(b) *Visual estimation of charges.*—In this method the charge of a fragment was estimated by visually comparing it with well identified fragments of comparable range and dip-angle. The charge of the HF was determined by visually inspecting the HF track and also its secondary decay products. This method is particularly useful when the HF track is quite steep and the track-width is difficult to perform. The error in the charge estimation is on the average one charge unit.

The charges of HFs, estimated by the above two methods, were compared, whenever possible, with the charges of uniquely identified HFs. The uniquely identified HFs were those, which gave correct binding energies and no other decay scheme was possible for the events (*see* Section 2.5 for analysis of these events). When the charge estimate for the HFs is not unique, equal weightage is given for the assigned charges of the HFs. In this way visual estimation of charge of HFs is found to be good in  $\approx 90\%$  of the cases. The charge spectrum of HFs obtained is shown in Fig. 2. The hatched portion of the histogram refers to mesic decay of HFs and the rest to non-mesic decay of HFs\*.

## 2.5. Analysis of Hyperfragments

(a) *Decay modes of  $\pi^-$  mesic HFs.*—Out of the 65 MHFs† obtained in this investigation only in 44 cases the pion could be brought to rest; in the remaining cases the pions left the stack or interacted in flight. In order to fit decay schemes the events were analysed on CDC-3600 computer. For

\* Possible cases of eleven  $\pi^0$  emission in the decay of HFs were not included in this histogram for NMHF decays.

† Two HFs that decayed by  $\mu^-$  and  $\pi^+$  modes are not included in this analysis; *see* reference (18).

this purpose the identity of the meson track was assumed to be due to a negative pion; as for the charges of the other prongs and that of HF track the maximum and minimum values permissible within the measuremental errors were assigned. All possible combinations for the decay schemes were then attempted by the computer. The unbalanced momentum was given to an invisible recoil or a neutron; if the unbalanced momentum was less than 100 MeV/c., the computer also tried decay schemes without any invisible recoil or neutron. The computer printed out all possible decay schemes where binding energies of HFs agreed to within three-standard deviation of the expected binding energies. In all these computations the mass values of various nuclei and particles were taken from König *et al.*,<sup>14</sup> and Rosenfeld *et al.*<sup>15</sup>

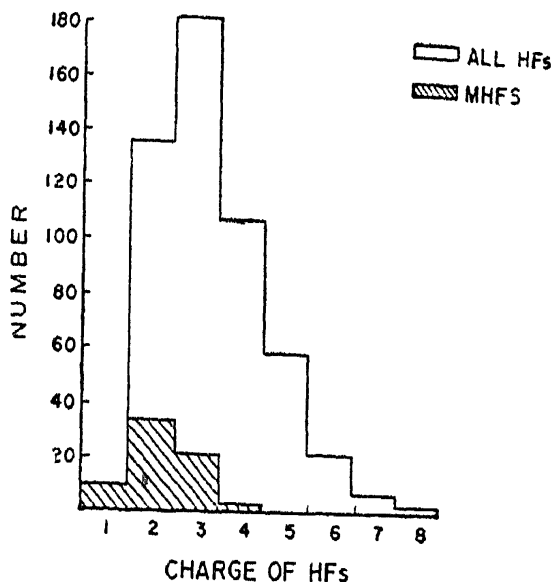


FIG. 2. The charge spectrum of HFs. The hatched portion refers to  $\pi^-$  mesonic HFs.

With the above computer analysis we could obtain unique decay schemes for 32 MHFs. Decay schemes and binding energies for these events are presented in Table II. These binding energies are in good agreement with those quoted by Burhop *et al.*<sup>17</sup>

(b) *Decay modes of non-mesic HFs.*—All non-mesic HFs have also been analysed by the CDC-3600 computer in the same way as is described in Section 2.5 (a); besides all that is described in 2.5 (a), the computer also tried decay schemes with a neutral pion whenever the total visible energy was  $\leq 10$  MeV.‡ In this way 11 possible  $\pi^0$  decays and 25 unique non-mesic decays have been identified; they are presented in Tables III (a) and III (b) respectively.

‡ An upper limit of 10 MeV has been chosen because it is known from mesic HFs that the total energy carried away by secondary charged particles other than the pion is, in general,  $\leq 10$  MeV.